Summary of the research funded by NKFI K-129249

Synergy of Wide-Field Surveys – Space and Ground

1. Introduction

Following the research proposal inherent to the grant, during the funding period (2018.09.01 - 2023.11.30) our study focused on the following main topics:

- *Synergies:* RR Lyrae stars: distances – pulsational and evolutionary vs Gaia; extrasolar planets: near infrared thermal emission and reflectivity; single transit resolution; refutal of a red nova candidate.
- *Other topics:* Code development for Kepler K2 – TRAN_K2; incidence rate of the Blazhko effect, systematic error in the RR Lyrae metallicities.

Highlighted results will be described in the corresponding sections. In Sect. 4 we estimate the impact of the studies carried out within this project. In the same section we also add notes concerning other grant-related activities, such as dissemination of the results.

As a general principle, we focus on results *directly* related to this project. In more practical terms, we do not discuss results associated more closely with NN-129075 (PI Johanna Jurcsik), even if they are impacting the respective field already (i.e., [12] on the companion mass distributions in binary RR Lyrae systems). Similarly, we do not highlight many-author papers, where the PI's contribution was less significant (e.g., photometric discovery of the scrutinized extrasolar planets – two planets among the seven presented in [11]).

2. Synergies

Following the nomenclature employed in the research proposal, here we focus on results more directly related to the synergy between the space- and ground-based observations. Nevertheless, some of the topics to be discussed in Sect. 3, will also have synergic aspects of the above type.

2.1 Resolving single transit ambiguities

This work addresses the question of single transits and the *recoverability of their periods* by combining the high-accuracy space data - hosting the single event, and the low-accuracy ground data - with multiple events. Traditional inverse variance weighting in the joint analysis would obviously not work, due to the much higher accuracy of the space data. Therefore, we opted for an optimization of the resulting BLS spectra (Kovacs et al. 2002) of the merged dataset, whereby we scanned the merging (i.e., weight) parameter α and accepted the value that maximized the SNR of the resulting BLS spectrum. The space data were assigned to weight α, whereas the ground data to $1 - \alpha$. The precise transit parameters derived from the single event space data were also utilized. More specifically, the following methods were tested:

- BLS0: All BLS parameters are free-floating while scanning α for the highest SNR spectrum.
- BLS1: As BLS0, but T_c (moment of the transit center) and T_{14} (transit duration) were fixed to the single transit values derived from the space data.
- BLS2: As BLS1, but we added also δ, the transit depth, again derived from the space data.
- BLS3: This is the spectrum inverse variance weighted combination of BLS0 and BLS1.

For a simple demonstration of the method at work, we generated a test signal on datasets compatible with the overall characteristics of a single sector TESS time series (Ricker et al. 2015), and an ideal ground-based survey with continuous coverage (like that of a single campaign K2 data). For simplicity, we assumed no gaps between the two datasets. The signal had a period of 35.123 d, with a transit depth of 0.3%. The ground-based data were assumed to be four times noisier, than the space data.

The left-hand panels in Figure 2.1.1 show the resulting BLS spectra from the various methods listed above. Interestingly, fixing all transit parameters (except for the period) yields rather poor result. We give a simple explanation for this phenomenon in the paper. The most favored method is BLS3, and we present ample amount of tests in the paper that support this assessment.

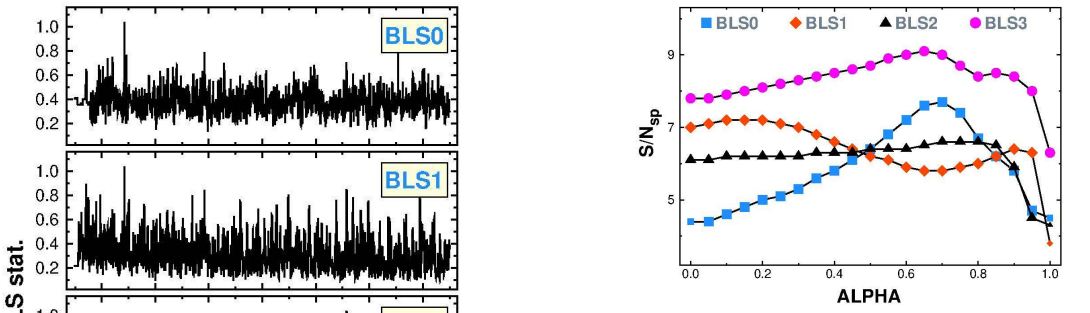

Fig. 2.1.1: *Left:* BLS spectra for a mock periodic transit signal generated on the timebase appropriate for the single sector TESS and a ground-based campaign, similar in extent than that of the K2 campaigns. The test signal has a period of 35.123 d, with a single event in the TESS set. The labels indicate the different methods used in the joint analysis of the two datasets (see text). *Right:* Dependence of the SNR of the BLS spectrum on the merging parameter α for the different merging methods.

2.2 Near infrared emissivity of two Hot Jupiters

WASP-121b: Near infrared observations of the secondary eclipse of the ultra hot Jupiter WASP-121b were made by the ANDICAM camera of the SMARTS Consortium[1] on three nights in 2016 and 2017. Although the expected depth of the eclipse was thought to be in the range of accessibility even for the 1.3 m telescope hosting the camera, the standard observational method (dither), supposed to handle the more severe CCD pixel inhomogeneities in the case of infrared cameras, made the detection rather challenging. Figure 2.2.1 explains why.

The dithering technique not only allows visiting various pixel regions and thereby averaging out their flaws, but the same procedure may also lead to using bad pixels, thereby leaving the result dependent on the chance selection of the dither positions. To cure this effect (shown in the middle of Fig. 2.2.1), we used a dither label-dependent first order polynomial correction together with a trapezoidal light curve model to jointly fit all available relative flux values. This procedure has

[1]The SMARTS Consortium allows anyone to request observations by its telescopes by paying for the telescope time. We covered the expenses from our earlier OTKA grant K-81373.

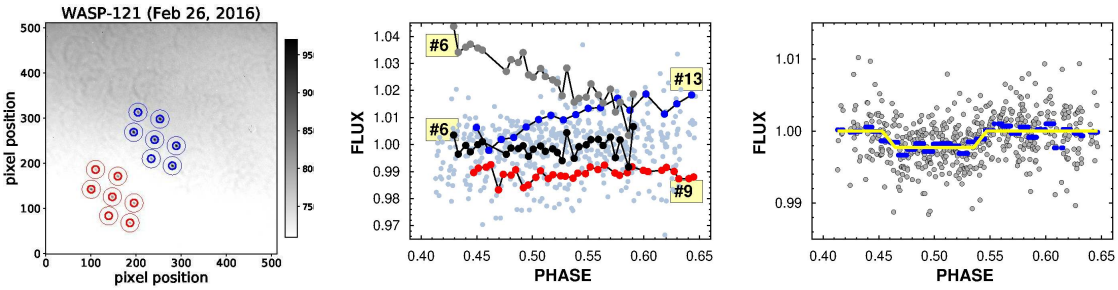

Fig. 2.2.1: *Left:* Composed image stamp of the $2.4' \times 2.4'$ field of view of the ANDICAM camera showing the 7 dither positions of WASP-121. Circles indicate the size of the apertures used for the measurements of the target and background fluxes (blue for the target and red for the comparison star). Each $15-20$ s exposure corresponds to one of the dither positions. *Center:* Simple flux ratios (pale dots, target over comparison star fluxes) folded by the orbital period of 1.27 d. Also shown are some of the flux values, belonging to a given dither position of a given night (i.e., #6, first night, #9, #13, second night). Dither #6 is shown with and without trend filtering. *Right:* The combined light curve after a full model fit, including instrumental systematics and trapezoidal-shaped eclipse signal. Blue dashes are for bin averages, yellow line is for the trapezoidal fit.

led to a huge improvement, and ultimately a 10σ detection of the secondary eclipse (right panel of Fig. 2.2.1).

From the above results we found (in agreement with other works) that the orbit is circular within the 1σ limit. The derived eclipse depth further supports the general trend of inefficient heat transport in most of the Hot Jupiters. As of this report, our measurement is the only one within the waveband range of $1.7-2.5\mu$m including one of the characteristic H_2O emission bands. The derived eclipse depth at 2.2μm provides an important anchor for atmospheric models using all available measurements in other wavelengths (Bourrier et al. 2020, Mikal-Evans et al. 2019, 2020).

WASP-5b: Our other target, WASP-5 was observed in 2011. We used the FourStar instrument, attached to the 6.5 m Baade telescope at the Las Campanas Observatory, Chile. We utilized the fast read-out capability of the instrument, and gathered data in the 2MASS K filter band in every 4.4 second. By using three comparison stars, with the aid of simple ensemble photometry, we detected the expected dip of the eclipse. After a linear trend filtering and jump correction due to sudden intermittent clouds, we got the light curve shown in the middle panel of Fig. 2.2.2. Then, two additional sets of data obtained from independent publications were combined with our data and a high-quality eclipse light curve (right panels in Fig. 2.2.2) was derived.

The exceptionally accurately measured deep eclipse of 2.70 ± 0.14 ppt excludes simple black body models at the 10σ level, but the flux is also higher (at the $5-7\sigma$ level), than current atmosphere models predict. By using data in the visual waveband, gathered by the TESS satellite from two sectors, we saw signatures of the eclipse signal that enabled us to estimate the geometric albedo, that turned out to be between 0.3 and 0.4 (depending on the degree of the atmospheric circulation). This value puts WASP-5b among the more reflective, infrequent Hot Jupiters. As presented in the paper, this planet is also an interesting candidate for further followup studies, due to the poor fit of the models to the Spitzer, and, in particular, to the more accurate data in the 2MASS band.

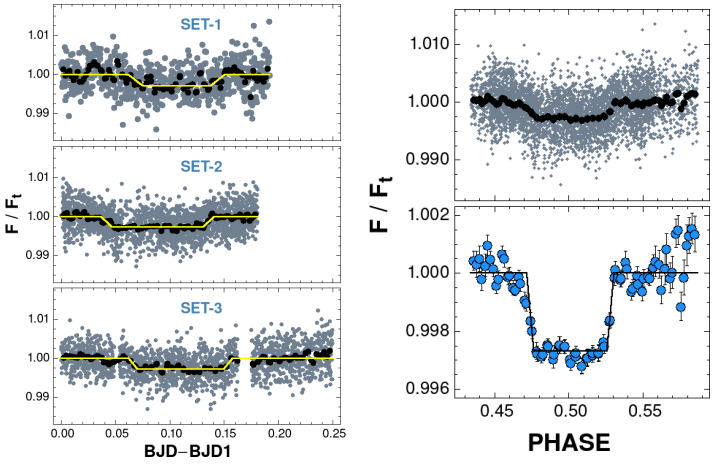

Fig. 2.2.2: *Left:* The three datasets used to generate the combined dataset of WASP-5 (see right panel). In each panel the abscissa shows the Baricentric Julian Date with respect of the moment of the first data point. Gray dots: unbinned fluxes; black dots: binned fluxes; yellow line: trapezoidal eclipse fit. The middle panel shows our observations by FourStar at the 6.5 m Baade telescope. *Right:* Combined, phase-folded light curve, using the three independent datasets shown in the left panel.

2.3 Consonance between the Gaia and theoretical RR Lyrae distances

In two consecutive papers ([17] and [18]) we examined the compatibility of the theoretical and directly derivable luminosities from the third (early) release of the Gaia parallaxes (EDR3). The "theoretical" luminosities involved linear pulsation and Horizontal Branch evolutionary models, combined with solid/simple observables (i.e., apparent magnitude, color, reddening and metallicity). In the case of double-mode RR Lyrae stars ([17]), due to the lack of trustable metallicities in the literature for these relatively faint stars, we had to estimated also [Fe/H]. This was possible, because the two observed periods yield additional constraints on the physical parameters, including the mass (and therefore [Fe/H]). It is important to note that the derived metallicities are probably quite reliable, because by using these metallicities in constructing the PLZ (period-luminosity-metallicity) relation for these RRd stars, we ended up a formula in a good agreement with the relations derived by different authors from separate samples of single-mode variables.

For the bright single (fundamental) mode field RR Lyrae stars there have been a large number of publications with accurate metallicities, so - after proper zero point corrections - we could use a large number of stars (156, instead of 30, like in the double-mode sample) for a straightforward testing the Gaia luminosities.

Figure 2.3.1 compares the Gaia and theoretical RR Lyrae luminosities for both classes of variables. As expected, the parallax error-ordered sub-samples of the single-mode stars show increased scatter around the identity lines. For the most accurate set A (62 stars), with relative parallax error less than 2%, the RMS of the luminosity difference is 0.03. The double-mode variables show the highest scatter - largely due to nearby blends at these faint magnitudes.

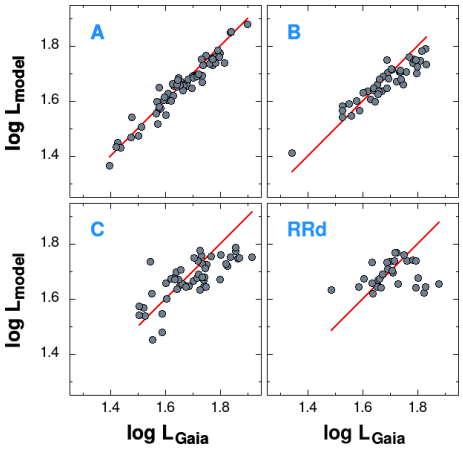

Fig. 2.3.1: Theoretical luminosities vs Gaia luminosities derived in [17] and [18]. The single-mode sample has been divided into three subsamples, with increasing RMS around the identity lines: 0.03, 0.04 and 0.06 for sets A, B and C, respectively. We used α-enhanced evolutionary models (solar-scaled models show the same scatter, but somewhat lower overall differences with respect to the Gaia luminosities). Double-mode stars are shown in the lower right corner.

2.4 KIC 9832227 is not a red nova precursor

The recently emerging class of red novae with outburst power between classical supernovae and novae attracted an increasing attention after the unique post discovery of nova V1309 Sco in the OGLE archive as a merging W UMa binary in its pre-blast phase (Tylenda et al. 2011). Following this exciting discovery, Molnar et al. (2017) suggested that the Kepler field star KIC 9832227 foresees similar fate by ~ 2022. Unfortunately, the followup investigation by Socia et al. (2018) - albeit with only a modest number of additional points in the O-C diagram - largely invalidated the above prediction. To further investigate the case of this object, we supplied additional O-C data by using ground-based photometric surveys of HATNet, ASAS and ASAS-SN, amateur observations from AAVSO and also data from the infrared satellite WISE.

In Fig. 2.4.1 we show the derived O-C diagram. The diagram clearly shows that the period of this 0.46 d period binary changes in a non-monotonic way. The pattern of the diagram indicates that a composite model that includes both cyclic and low-order secular variations will likely give a better fit. Indeed, as shown in the panels of Fig. 2.4.2, this model yields a very good fit, although even this ~ 20 years long dataset is too short to predict (accurately enough) the behavior of the system for the next several years.

The above mathematical description of the data suggests a hiarerchical system, where there is a third companion with an upper limit of $\sim 0.5 M_{\odot}$ on its mass and orbital period of ~ 5000 d. Although the recent analysis of the Gemini-N/'Alopeke speckle images by Salinas & Howell (2023) excludes any non-degenerate object above ~ 10 AU, our suggested model may still be valid, because of the estimated ~ 8 AU distance and the likely degenerate nature of the outer companion.

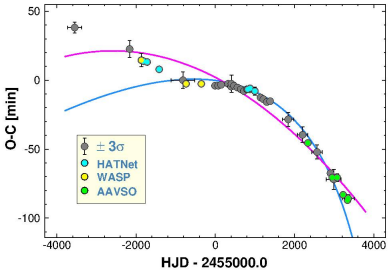

Fig. 2.4.1: O-C diagram for KIC 9832227, The compact set of gray dots in the middle comes from the Kepler satellite, while the single gray point with large error bars at -800 comes from the WISE satellite. Other points (including the gray ones) come from various ground-based sources). Neither the best-fit parabola (magenta), nor the earlier (also parabolic) model of Molnar et al. (2017) match well the data.

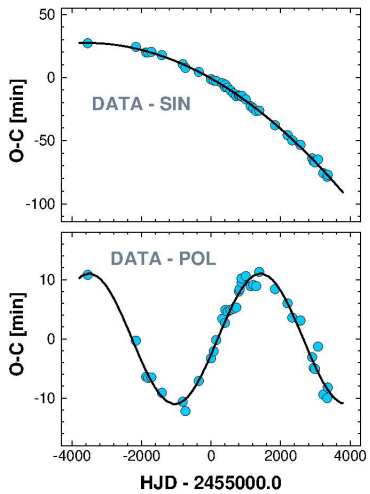

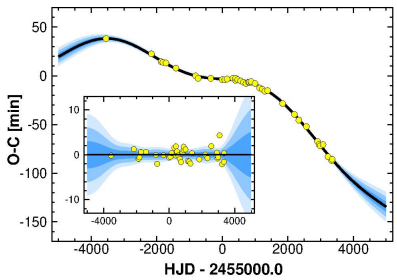

Fig. 2.4.2: *Left:* Decomposition of the O-C curve shown in Fig. 2.4.1 into a parabolic and a sinusoidal component. *Right:* The combined (parabola+sinus) fit (black line) to the observed O-C values. The various shades indicate the ranges of the predicted values from the fit (at the $1-3\sigma$ levels from dark to light shades). Stemming from the time scale of the variation, the inset shows the limited validity of the present model.

3. Other/related topics

3.1 tran_k2

In this work we introduced a new code to treat both instrumental systematics and stellar variability to filter out the time series before searching for periodic transit signals. Although the code was specified to the Kepler K2 time series, the design is general, and is applicable to any, "almost" continuous time series. The main ingredients of the code are as follows:

- TFA and EPD for systematics (Kovacs et al. 2005; Bakos et al. 2010);
- Detuned high-order Fourier fit with frequencies $\{k\alpha/T\}$, where $k = 1, 2, ..., m$, T is the total time span, and α is the detuning parameter, to minimize the Gibbs oscillations near the end points. We also discussed possible optimization for choosing the Fourier order m.
- Search for transit signal by BLS, and perform a full model fit to minimize the signal depressing effect of the filtering before the transit search.

We applied the method on the #5 campaign field of the K2 mission, and found that the code performed quite competitively with respect to the other codes developed for the same purpose by various research groups. Even more encouragingly, we found over 10 additional planet candidates that were not listed in the extrasolar planet catalogs, but were spotted with a high significance by our code. Figure 3.1.1 shows one of these new candidates.

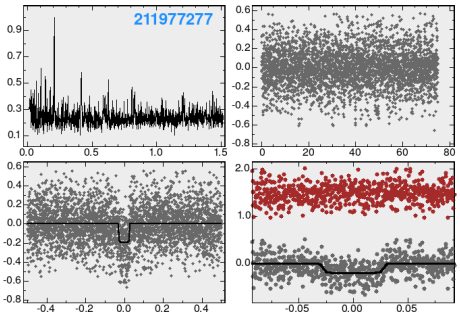

Fig. 3.1.1: EPIC 211977277, one of the several new planet candidates found in K2 field #5 by using TRAN_K2. *Upper left:* BLS spectrum, normalized, frequency is in d^{-1}; *Upper right:* TFA/FOUR-filtered time series, with [ppt] and [d] units on the Y and X axes, respectively; *Lower left:* Light curve folded with P=4.800 days and plotted in the full phase interval; *Lower right:* As on the left, but zoomed on the transit. The colored points are the residuals, shifted upward for better visibility.

3.2 Blazhko modulation is a general phenomenon

In an earlier paper (Kovacs, 2018), we analyzed the RR Lyrae stars in the K2 fields $01 - 04$. We developed a code that employs a proper filtering of both instrumental systematics and large amplitude, monomode (i.e., single period) stellar pulsation (the method uses several aspects of the code TRAN_K2 (see Sect. 3.1). Earlier (and also current) studies on Kepler/K2 variables either use uncorrected SAP (or similar), or processed PDC (or similar) fluxes (e.g., Plachy et al., 2019; Benkő et al., 2014). In these and similar applications the systematics are not properly filtered out and, if filtering happens at some degree, the procedure oppresses also part of the small signals, thereby making more difficult to detect them. In addition, no good estimation can be made on the signal component without full modeling (see Kovacs et al. 2005).

Because the code we employed handles the effects above, we were able to go deeper in the residual signal search. In this conference proceedings we present an extended work of Kovacs (2018) and confirm the finding of that paper: the observed rate of Blazhko phenomenon is about 90%, and, considering observational bias due to high noise, the true incidence rate is likely close to 100%.

An example of low-amplitude Blazhko modulation is displayed in Fig. 3.2.1. The detection in two overlapping campaign fields and the high S/N show that the detection is significant. On the

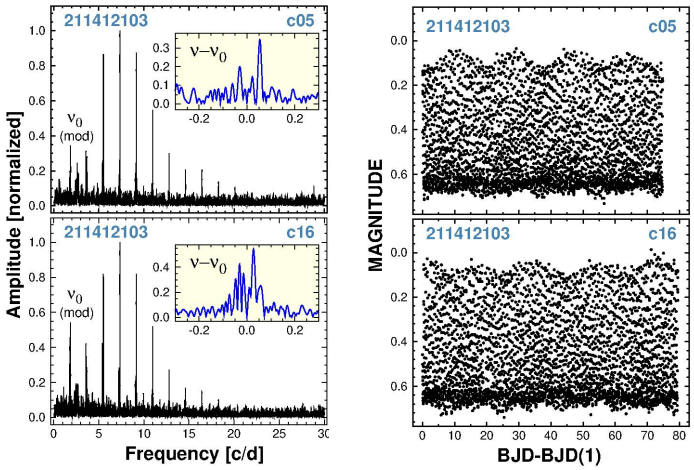

Fig. 3.2.1: *Left:* Fourier spectra of EPIC 211412103 from two different K2 fields after prewhitening by the main pulsation component and its harmonics. Please note that the modulation is stronger at higher harmonics. *Right:* Light curves after filtering out the systematics due to the wobble of the spacecraft. The low-amplitude Blazhko modulation is clearly visible in both datasets of the different campaigns.

other hand, traditional data processing may lead easily to overlook cases like this (Plachy et al., 2019).

3.3 Systematic error in RR Lyrae metallicities

The standard procedure employed for the determination of stellar chemical abundances via theoretical or template spectrum fits to the observed spectra, suffer from parameter degeneracy, most importantly, through the correlation with the gravity (e.g., Thévenin & Idiart, 1999). In the case of dynamical atmospheres (e.g., in RR Lyrae stars), there is also the effect of changing physical conditions, further increasing the degree of ambiguity both on the theoretical (LTE vs non-LTE) and on the observational side (e.g., catching the proper phase, close to the static atmospheric conditions). While the changing atmospheric conditions complicate the chemical analysis, classical radial pulsators offer also a precise, time-dependent determination of the temporal value of the gravity, thereby eliminating an important degeneracy in the abundance determination.

In the paper we show the existence of the above correlation for RR Lyrae stars (see Fig. 3.3.1), and on the basis of this finding, we give simple correction formulae for the derivation of more accurate iron abundances from the already published ones (including some of the big surveys, e.g., LAMOST). At the same time, we recommend using the 'in situ' determination of the gravity (much in line followed by Clementini et al. 1995 and Lambert et al. 1996), to obtain more accurate abundances without the need for post-correction, as described in the paper.

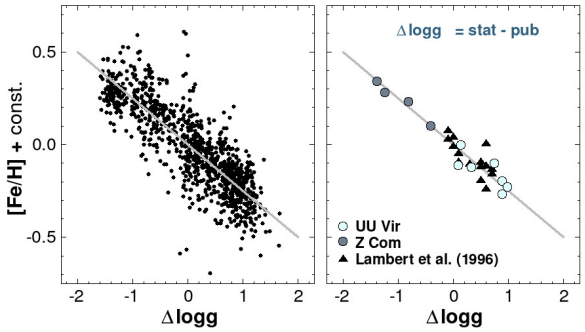

Fig. 3.3.1: Correlation between $\Delta \log g$ (static minus spectroscopic $\log g$) and the published spectroscopic iron abundance [Fe/H] (shifted by the average target-by-target metallicities). *Left:* Full sample of 197 stars with multiple spectra. *Right:* Example of two well-fit cases and the RR Lyrae set from Table 3 of Lambert et al. (1996) with "photometric" and "spectroscopic" metallicities, confirming the correlation discussed in [28].

4. Scientific impact and related activities

In the funding period we produced 28 publications, among which 22 appeared in refereed journals and the rest in the form of conference proceedings (also available at the NASA/ADS depository). We received altogether 84 independent citations on these works at the time of this report.

The following list briefly indicates the potentials of the particular results in affecting the respective fields of the studies.

- *Gaia parallaxes for RR Lyrae stars:* Based on independent theoretical considerations, they are in good agreement up to a possible offset of ~ 0.02 mas for fainter stars - [17], [18].
- *Metallicity scale for RR Lyrae stars:* They suffer from a systematic error of several tenths of dex due to the strong correlation between the spectroscopic gravity and [Fe/H]. We suggest the revision of those metallicities by incorporating the measured/estimated temporal gravities from the radial velocity data - [28].
- *Incidence rate of the Blazhko effect:* By extending our earlier study to K2 fields $01-08$ (788 stars) we show that the observed incidence rate is about 90%, implying close to 100% true rate - [16].
- *Thermal emission of two exoplanets:* We measured the near infrared ($2\mu m$) emission for WASP-121b (the first measurement of this kind for this ultrahot planet). For the classical Hot Jupiter WASP-5b, we combined our $2\mu m$ occultation light curve with two, already published light curves. The merging has led to a 5% outstanding precision in the determination of eclipse depth.
- *Transit search code for K2:* By utilizing the Fourier method for filtering out stellar variability and Trend Filtering Algorithm (TFA) for handling instrumental systematics, we devised a new complex FORTRAN code to search for transiting extrasolar planets in the Kepler K2 fields. The code is powerful, and competitive with the most efficient methods available.

The PI presented the following talks on various occasions.

4.1 Seminar:

- *Detecting Extrasolar Planets*; Department of Astronomy, Comenius University, Bratislava, 2018.12.13 [host: Jan Budaj]

4.2 Invited talk:

- *RR Lyrae pulsation and evolutionary models tested against Gaia EDR3*; "Stellar evolution along the HR diagram with Gaia", MW-Gaia WG2/1 Hybrid Workshop, Naples, Italy, 2022.09.20-23
  `https://indico.ict.inaf.it/event/2023/timetable/#20220921.detailed`

4.3 Contributed talks:

- *From Single to Multiple Transits*; "PLATO ESP2019: Single, shallow and strange transits", University of Warwick, UK, 2019.09.2-4
  `https://platomission.com/category/meetings/`
- *On the Incidence Rate of Blazhko Stars*; "RR Lyrae/Cepheids 2019: Frontiers of Classical Pulsators – Theory and Observations" Cloudcroft, New Mexico, USA, 2019.10.13-18
  `https://www.aspbooks.org/a/volumes/table_of_contents/?book_id=597`

- *Debiasing Observed Blazhko Occurrence Rates*; "Large-scale surveys as bridges between spectroscopy and photometry" La Palma, Spain, 2022.09.26-30
`https://meetings.iac.es/RRLCep2022/pages/programme.php`

Other members (Janos Nuspl and Johanna Jurcsik), presented posters at the New Mexico meeting in 2019.

References[2]

[01] Csörnyei, Geza & Szabados, Laszlo: 2019, *Astrophys. and Space Sci.*, **364**, 151

[02] Jurcsik, J.: 2019, *MNRAS*, **485**, 5897

[03] Kovacs, Geza: 2019, *A&A*, **625**, A145

[04] Kovacs, Geza & Kovacs, Tamas: 2019, *A&A*, **625**, 80

[05] Kovacs, Geza, Hartman, Joel D., Bakos, Gaspar, Á.: 2019, *A&A*, **631**, A126

[06] Szabados, Laszlo: 2019, *Contrib. Astron. Obs. Skalnate Pleso*, **49**, 171

[07] Zhou, G. et al.: 2019, *AJ*, **158**, 141

[08] Kovacs, Geza: 2020, *A&A*, **643**, A169

[09] Nuspl, J., Hajdu, T., Hegedus, T.: 2020, *Contrib. Astron. Obs. Skalnate Pleso*, **50**, 419

[10] Tarczay-Nehez, D., Szabados, L., Dencs, Z.: 2020, in *Conference Proceedings*[3]

[11] Bakos, G. Á. et al.: 2021, *AJ*, **162**, 7

[12] Hajdu, Gergely, et al.: 2021, *ApJ*, **915**, 50

[13] Jurcsik, J., Hajdu, G., Juhasz, A.: 2021, *MNRAS*, **505**, 2468

[14] Jurcsik, J., Sodor, A., Bognar, Zs.: 2021, *ASPC*, **529**, 327

[15] Jurcsik, J., Szabo, P., Prudil, Z., Skarka, M., Hajdu, G.: 2021, *ASPC*, **529**, 329

[16] Kovacs, G.: 2021, *ASPC*, **529**, 51

[17] Kovacs, Geza & Karamiqucham, Behrooz: 2021, *A&A*, **653**, A61

[18] Kovacs, Geza & Karamiqucham, Behrooz: 2021, *A&A*, **654**, L4

[19] Nuspl, J.: 2021, *ASPC*, **529**, 336

[20] Csörnyei, G. et al.: 2022, *MNRAS*, **511**, 2125

[21] Jurcsik, Johanna & Juhasz, Aron: 2022, *MNRAS*, **517**, 1907

[22] Kovacs, G. et al.: 2022, *A&A*, **664**, A47

[23] Cseh, B. et al.: 2023, *A&A*, **(in press)**

[24] Healy, B. F., McCullough, P. R., Schlaufman, K. C., Kovacs, G.: 2023, *ApJ*, **944**, 39

[25] Jurcsik, Johanna & Hajdu, Gergely: 2023, *MNRAS*, **525**, 3486

[27] Kovacs, Gabor, B., Nuspl, Janos, Szabo, Robert: 2023, *MNRAS*, **521**, 4878

[26] Kovacs, Gabor, B., Nuspl, Janos, Szabo, Robert: 2023, *MNRAS*, **(in press)**

[28] Kovacs, Geza & Jurcsik, Johanna, 2023, *A&A*, **678**, 138

Bakos, G. Á., Torres, G., Pál, A. et al. 2010, *ApJ*, **710**, 1724

Benkő, J. M., Plachy, E., Szabó, R. et al. 2014, *ApJS*, **213**, 31

Bourrier, V., Kitzmann, D., Kuntzer, T. et al. 2020, *A&A*, **637**, A36

Clementini, G., Carretta, E., Gratton, R. et al. 1995, *AJ*, **110**, 2319

Kovács, G., Zucker, S. & Mazeh, T., 2002, *A&A*, **391**, 369

Kovacs, G., Bakos, G. & Noyes, R. W. 2005, *MNRAS*, **356**, 557

[2]Numbered publications are the ones which acknowledge this grant (NKFI K-129249). Papers with more than five authors are referred to with the first author only.

[3]The exact reference is as follows: *"Stars and their Variability Observed from Space"*, Vienna, Aug. 19-23, 2019. Eds.: C. Neiner et al., p. 115

Kovacs, G. 2018, *A&A*, **614**, L4
Lambert, D. L., Heath, J. E., Lemke, M., et al. 1996, *ApJS*, **103**, 183
Mikal-Evans, T., Sing, D. K., Goyal, J. M. et al. 2019, *MNRAS*, **488**, 2222
Mikal-Evans, T., Sing, D. K., Kataria, T. et al. 2020, *MNRAS*, **496**, 1638
Plachy, E., Molnár, L., Bódi, A. et al. 2019, *ApJS*, **244**, 32
Ricker, G. R., Winn, J. N., Vanderspek, R., et al. 2015, *JATIS*, **1**, 014003
Salinas, R. & Howell, S. B. 2023, *RNAAS*, **7**, 75
Socia, Q. J., Welsh, W. F., Short, D. R. et al. 2018, *ApJ*, **864**, L32
Thévenin, F. & Idiart, T. P. 1999, *AJ*, **521**, 753
Tylenda R., Hajduk M., Kamiński T. et al. 2011, *A&A*, **528**, A114